Modeling multiwavelength afterglows detected from the VHE-GRB population with NAIMA

Monica Barnard[1], Ankur Ghosh[1], Jagdish C. Joshi[2], Soebur Razzaque[1,3,4]

[1]Centre for Astro-Particle Physics (CAPP), Department of Physics, University of Johannesburg, Auckland Park 2006, South Africa
[2]Aryabhatta Research Institute of Observational Sciences (ARIES), Manora Peak, Nainital 263001, India
[3]Department of Physics, The George Washington University, Washington, DC 20052, USA
[4]National Institute for Theoretical and Computational Sciences (NITheCS), South Africa

11th International Fermi Symposium, 9-13 September 2024, College Park, Maryland, USA

Gamma-ray burst (GRB) evolution

Dado et al. (2022)

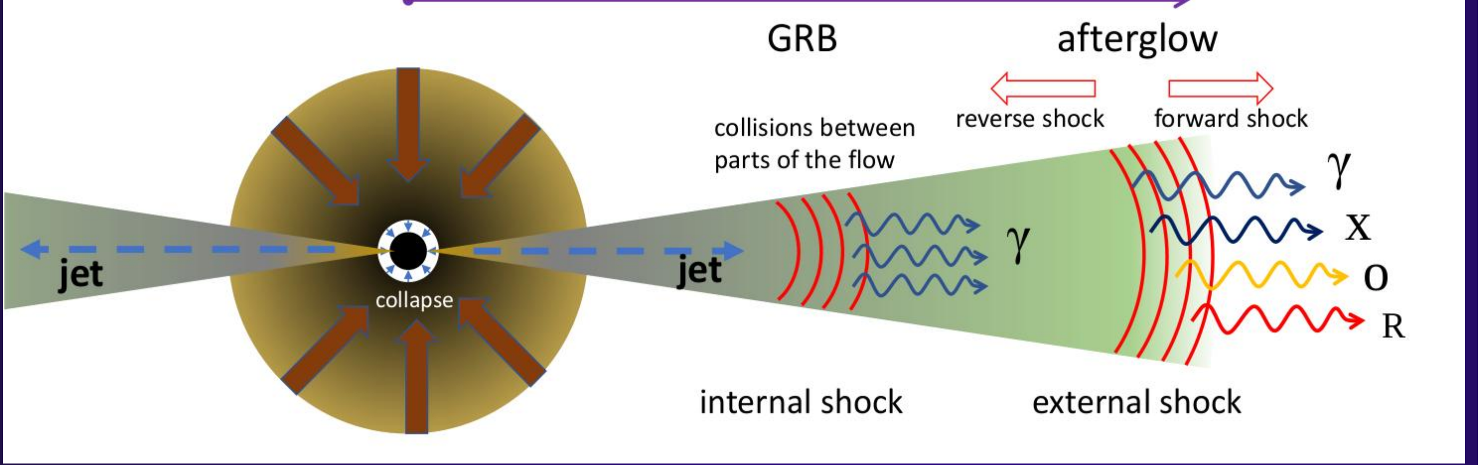

GRB emission from the jet → **Free -coasting phase of the blastwave** → **Declaration of the blastwave** → **Self-similar solution of blastwave**

Formation

- Classification of GRBs
- Structure of jet - fireball model.

Blast wave evolution with time:

- Internal / external shocks.
- Prompt to afterglow emission over multiple wavebands.
- Information about, e.g., explosion energy (isotropic energy E_k), surrounding environment (density n, Lorentz factor Γ, composition), magnetic field strength, and jet properties (angle, velocity).
- Afterglow observations assist in understanding the physics of GRBs, their progenitors, and the extreme conditions involved.

Multiwavelength afterglow observations

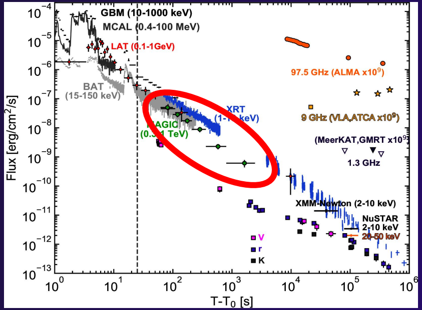

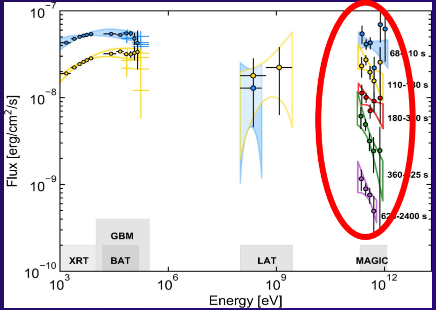

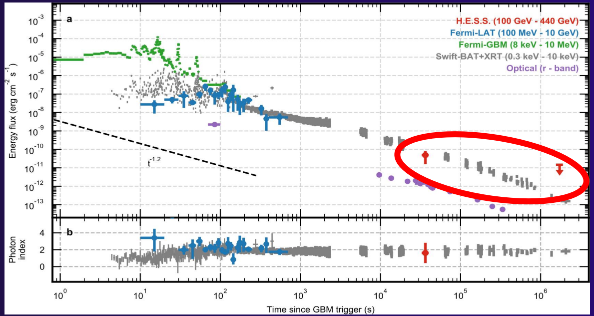

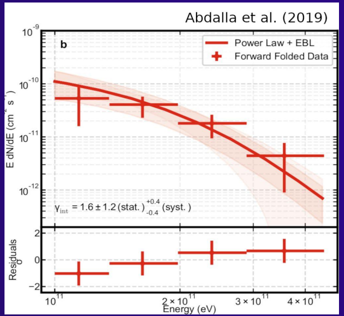

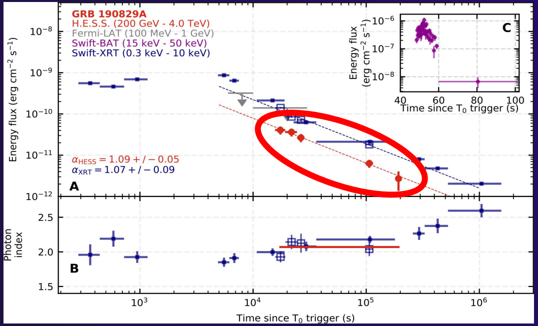

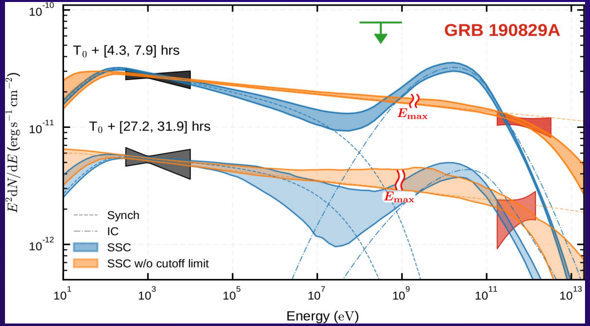

- **GRB 221009A** (Huang et al., 2022)
  T_{90} = 600 s, 10σ, z = 0.151, E_k~10^{54} erg.
  Up to E~13 TeV reported by LHAASO.
- **GRB 190114C** (Acciari et al., 2019)
  T_{90} = 116 s, 50σ, z = 0.4245, E_k~10^{53} erg.
  Detected at 300 GeV < E < 1 TeV by MAGIC. Prompt emission.
- **GRB 180720B** (Abdalla et al., 2019)
  T_{90} = 48.9 s, 5σ, z = 0.653, E_k~10^{53} erg.
  Up to E~440 GeV detected by H.E.S.S., 10 hrs after initial burst.
- **GRB 190829A** (Abdalla et al., 2021)
  T_{90} = 63 s, 20σ, z = 0.0785, E_k~10^{50} erg.
  Up to E~3.3 TeV detected by H.E.S.S., 5 hrs and 30 hrs after initial burst.

Other:

- **GRB 201015A** (Blanch et al., 2020)
  z = 0.426, >3σ
  Observed at 50 GeV < E < 50 TeV by MAGIC.
- **GRB 201216C** (Abe et al., 2024)
  z = 1.1, >5σ
  E > 70 GeV detected by MAGIC.
- **GRB 160821B** (Acciari et al., 2021)
  z = 0.162, 3σ
  E > 0.5 TeV detected by MAGIC.

Modelling afterglow emission

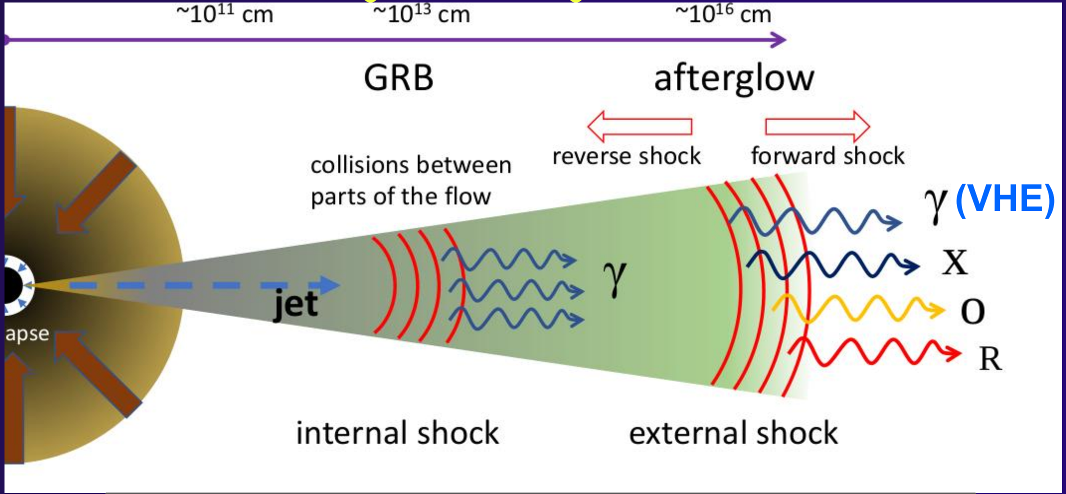

$$f(E) = \exp\left(-\frac{E}{E_c}\right)\begin{cases} A(E/E_0)^{-\alpha_1} & : E < E_b \\ A(E_b/E_0)^{\alpha_2-\alpha_1}(E/E_0)^{-\alpha_2} & : E > E_b \end{cases}$$

- η_e: the fraction of energy available as non-thermal electrons
- E_{break}: energy of the break in the electron distribution
- α_2: the power law index above the break in the electron distribution
- E_{cut}: cut-off energy of the electron distribution
- B: the intensity of the magnetic field

Blandford & Mckee (1976); Meszaros & Rees (1997)

Motivation for study:

- **Similarity between the VHE detected GRBs**
- **Establish a correlation with other GRBs**

GRB physics in NAIMA
Zabalza (2015)
https://naima.readthedocs.io/en/

- Compute non-thermal radiation from relativistic particle populations: *electrons*.
- Particle distribution: *Exponential Cutoff Broken Power Law.*
- Blastwave evolution in two environments: *wind / ISM.*
- Radiative models to explain afterglow: *Synchrotron / Inverse Compton (IC) scattering / SSC.*
- Because of the synchrotron cutoff limit, explosion detected in the VHE regime is expected to be IC origin.

Modelling afterglow emission

GRB emission from the jet → **Free -coasting phase of the blastwave** → **Declaration of the blastwave** → **Self-similar solution of blastwave**

- ❑ Calculation of the Lorentz factor of the forward shock

$$\Gamma^2 = \frac{E_{iso}}{Mc^2}$$

- ❑ Radius of the shock front can be calculated using both evolution scenarios

$$R \simeq \Gamma^2(R)c\Delta t \begin{cases} 8 & \text{for ISM} \\ 4 & \text{for wind}\,, \end{cases}$$

- ❑ Lorentz factor for ISM

$$\Gamma = \left(\frac{1}{8}\right)^{3/8} \left(\frac{3E_{iso}}{4\pi n m_p c^2 (c\Delta t)^3}\right)^{1/8}$$

- ❑ Lorentz factor for wind

$$\Gamma = \left(\frac{3E_{iso}v}{4c^3\Delta t\dot{m}}\right)^{1/4}$$

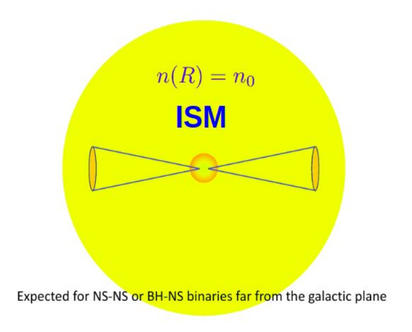

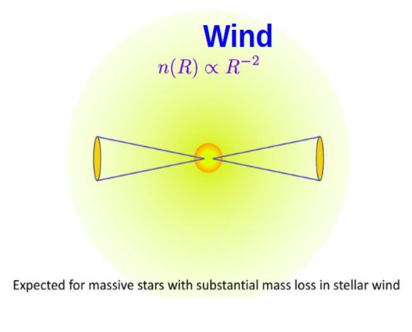

GRB physics in NAIMA
Zabalza (2015)
https://naima.readthedocs.io/en/

- ❑ Compute non-thermal radiation from relativistic particle populations: *electrons*.
- ❑ Particle distribution: *Exponential Cutoff Broken Power Law.*
- ❑ Blastwave evolution in two environments: *wind / ISM*
- ❑ Radiative models to explain afterglow: *Synchrotron / Inverse Compton (IC) scattering / SSC*

Modelling afterglow emission

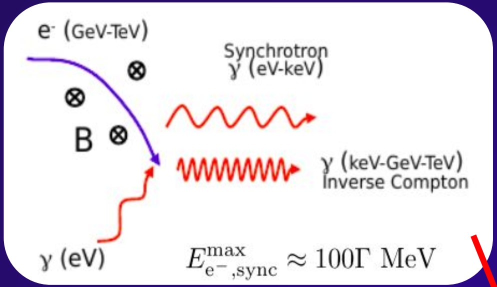

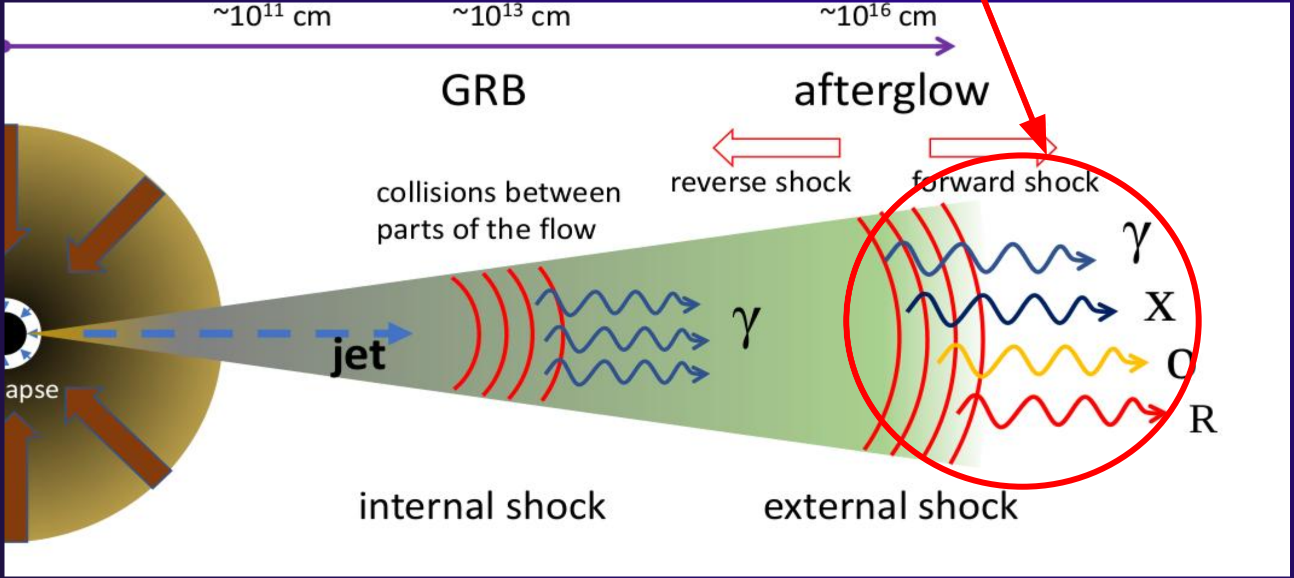

Dado et al. (2022)

GRB physics in NAIMA Zabalza (2015)
https://naima.readthedocs.io/en/

- Compute non-thermal radiation from relativistic particle populations: *electrons*.
- Blastwave evolution in two environments: *wind / ISM.*
- Particle distribution: *Exponential Cutoff Broken Power Law.*
- Radiative models to explain afterglow: *Synchrotron / Inverse Compton (IC) scattering / SSC.*
- Wang et al. (2019), Joshi & Razzaque (2021), Derishev & Piran (2021), Klinger et al. (2023)
- Because of the synchrotron cutoff limit, explosion detected in the VHE regime is expected to be IC origin

Modelling afterglow emission

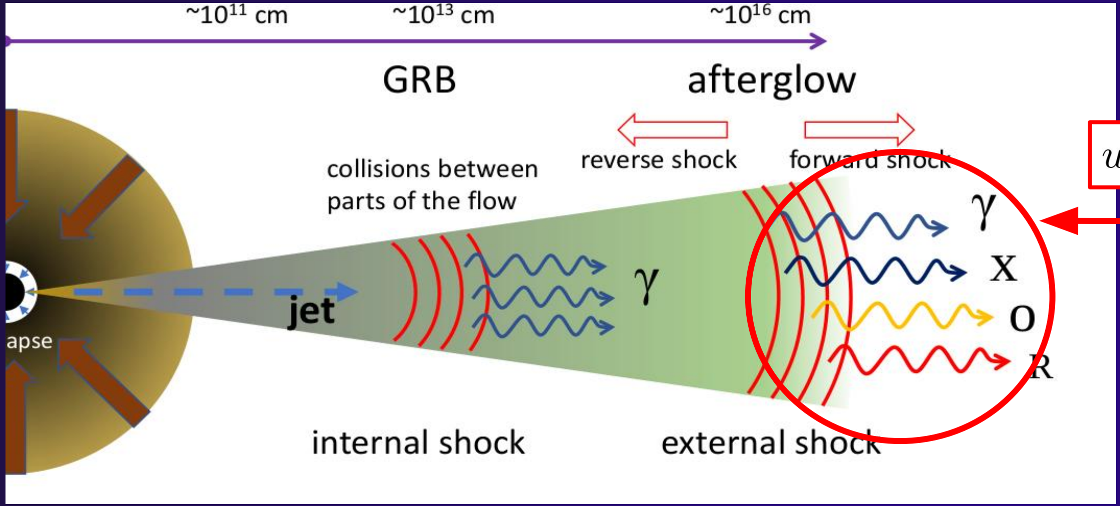

$$u_{\rm ex} \geq 4n(R)m_p c^2 \epsilon_B$$

$$\frac{dN}{dE} = \left(\frac{dN}{dE}\right)_{\rm EC} e^{-\tau(E,z)} = \left(\frac{L}{4\pi D_{\rm L}^2}\right)_{\rm EC} e^{-\tau(E,z)}$$

GRB physics in NAIMA
Zabalza (2015)
https://naima.readthedocs.io/en/

- ***Implementations***:
  - External Compton (EC) - seed photon field (CMB / far- and near-infrared
  - EBL attenuation - method taken from Barnard et al. (2024)
- ***EC dominance:*** energy density of external photons greater than magnetic field!!
- MCMC
- Energy spectra vs time

Time evolution of multiwavelength SEDs GRB 190114C

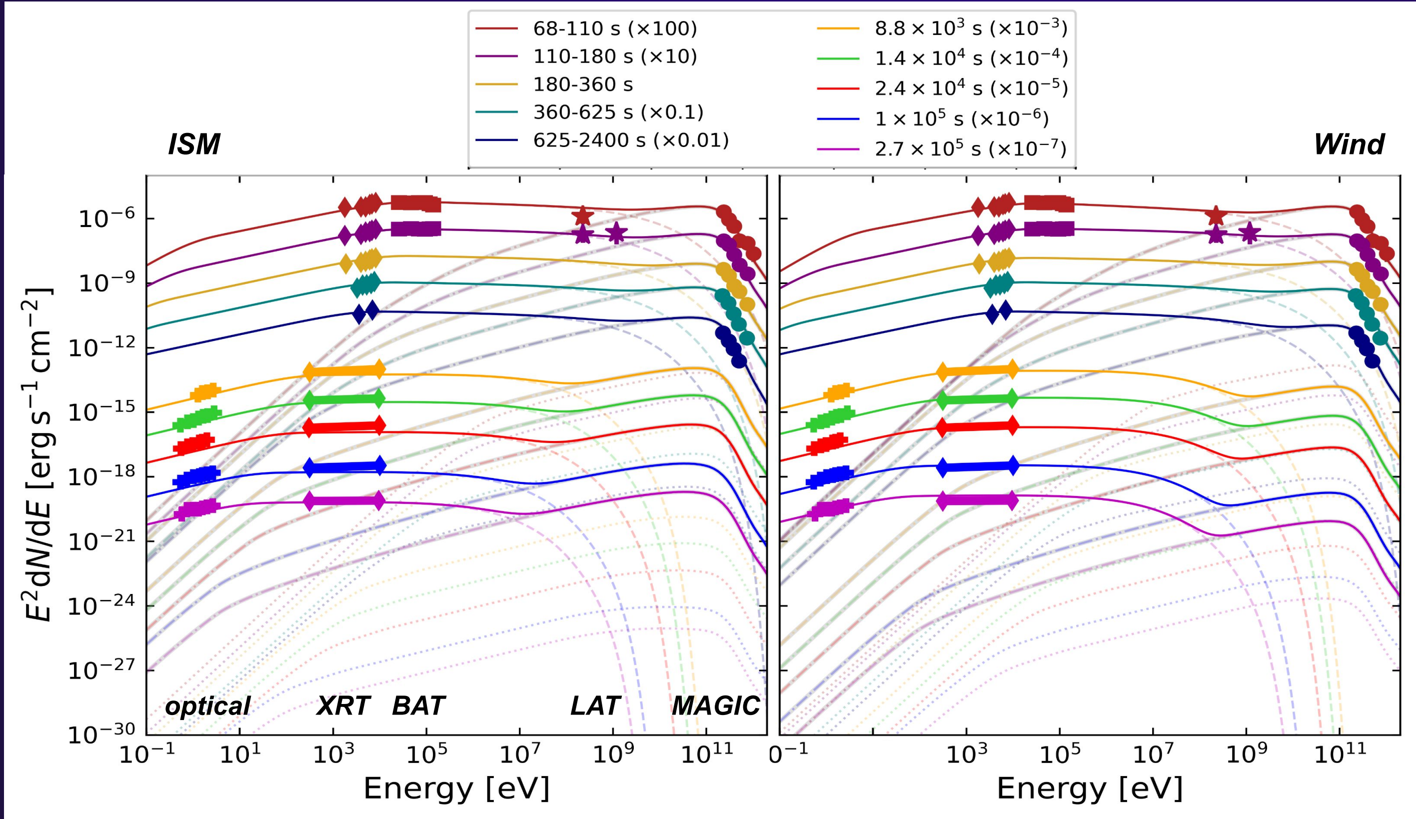

- Evolution of energy spectra over several epochs.
- Energies from optical to VHE gamma-rays.
- MCMC method for epoch 110-180 s.
- Data collected from Acciari et al. (2019) and https://www.swift.ac.uk/.
- SSC and EC emission combined.

Time evolution of multiwavelength SEDs GRB 221009A

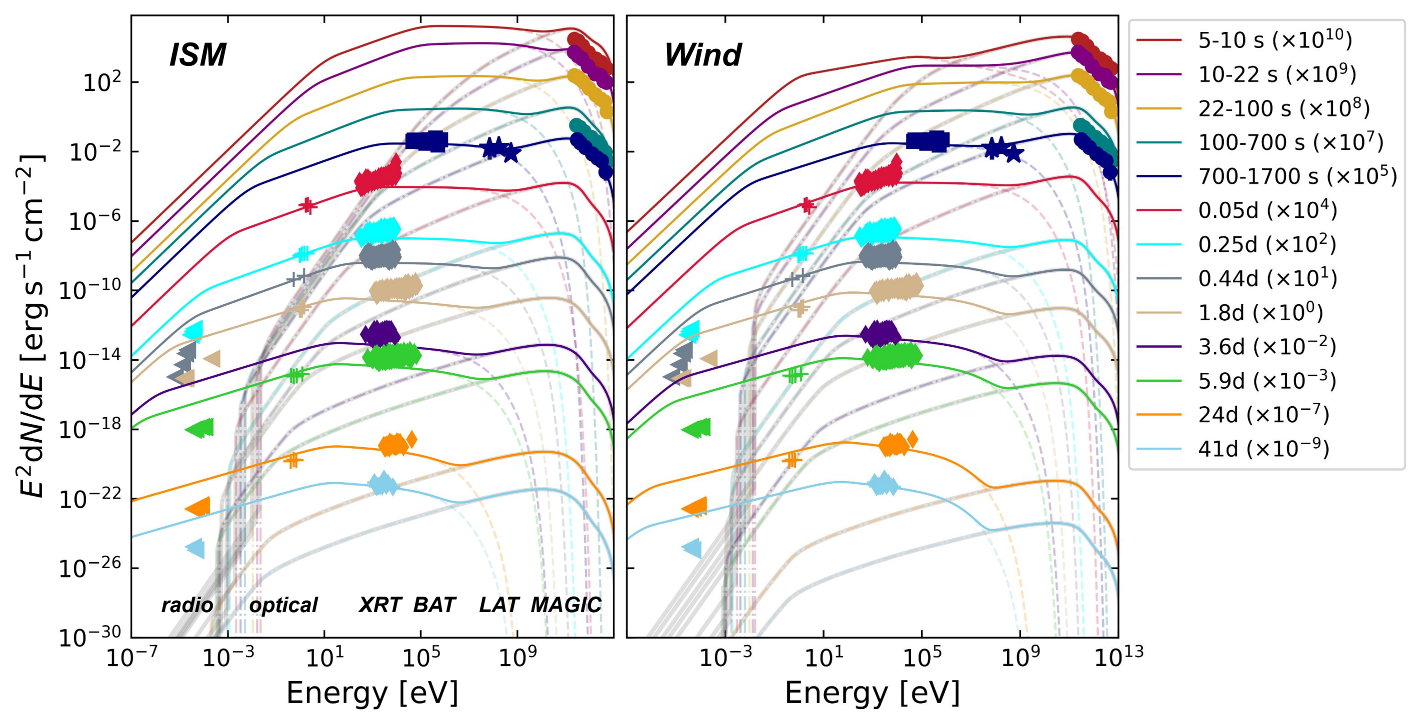

- Evolution of energy spectra over several epochs.
- Energies from optical to VHE gamma-rays.
- MCMC method for epoch 700-1700 s.
- Data collected from Ren et al. (2024), Banerjee et al. (2024).
- SSC and EC emission combined.
- EC component was omitted for figure clarity.

Time evolution of multiwavelength SEDs GRB 180720B

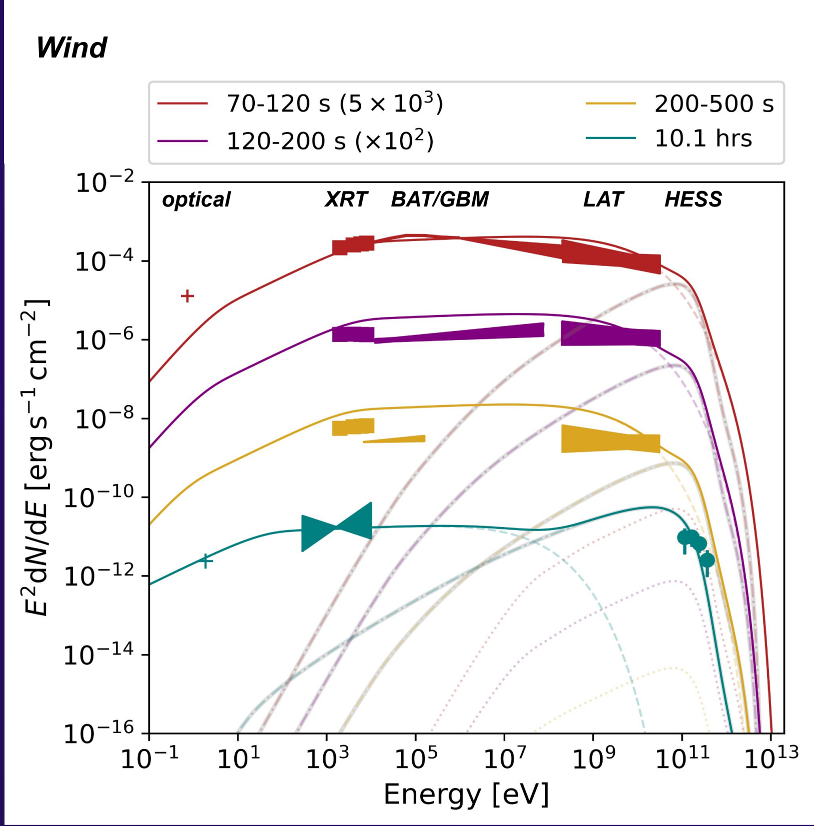

- Evolution of energy spectra over several epochs.
- Energies from optical to VHE gamma-rays.
- MCMC method for epoch 10.1 hrs.
- Data collected from: Abdalla et al. (2021), Ronchi et al. (2020). Fraija et al. 2019), https://www.swift.ac.uk/.
- X-ray - extrapolation to the time window of H.E.S.S. observation,
- The EC emission significantly lower.

Time evolution of multiwavelength SEDs GRB 190829A

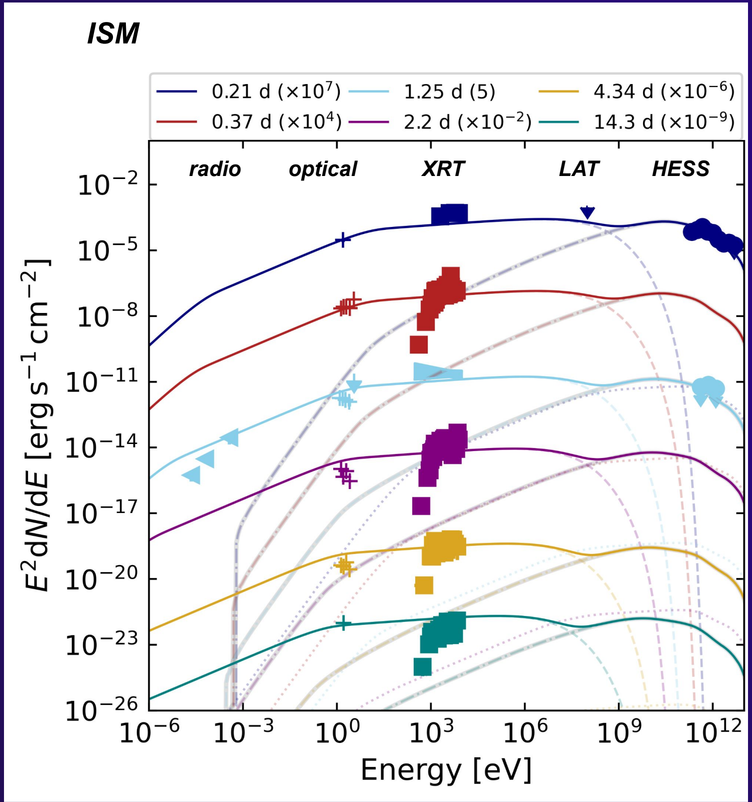

- Evolution of energy spectra over several epochs.
- Energies from optical to VHE gamma-rays.
- MCMC method for epoch 0.21 d (a.k.a night 1 *HESS* detection).
- Data collected from: Abdalla et al. (2021), Hu et al. (2020), Salafia et al. (2021), https://www.swift.ac.uk/.
- The EC emission was omitted for figure clarity.

Summary of model parameters

Parameter	GRB 180720B	GRB 190829A	GRB 190114C		GRB 221009A	
	Wind	*ISM*	*ISM*	*Wind*	*ISM*	*Wind*
E_k (erg)	3.5×10^{53}	1×10^{52}	8×10^{53}	8×10^{53}	3.5×10^{54}	5×10^{54}
Γ	7	5	64.6	83.4	33.4	38.8
$\dot{M}_w$ ($M_\odot$/yr)	1×10^{-4}	–	–	5×10^{-6}	–	8×10^{-5}
v_w (cm/s)	10^8	–	–	10^8	–	10^8
n_w (cm^{-3})	34	–	–	3.45	–	51.6
n_0 (cm^{-3})	–	30	10	–	15	–
p	$2.0^{+0.6}_{-0.4}$	$1.79^{+0.09}_{-0.09}$	$2.07^{+0.10}_{-0.09}$	$2.07^{+0.12}_{-0.09}$	$1.85^{+0.01}_{-0.03}$	$1.87^{+0.19}_{-0.02}$
ϵ_e	$0.028^{+0.06}_{-0.001}$	$0.038^{+0.005}_{-0.005}$	$0.016^{+0.001}_{-0.001}$	$0.012^{+0.001}_{-0.001}$	$0.009^{+0.003}_{-0.002}$	$0.006^{+0.013}_{-0.002}$
ϵ_B	3×10^{-4}	1×10^{-4}	1.5×10^{-3}	1.2×10^{-3}	1.6×10^{-4}	4.3×10^{-5}
B (G)	$0.34^{+0.4}_{-0.19}$	$0.11^{+0.3}_{-0.2}$	$2.4^{+0.3}_{-0.2}$	$2.5^{+0.3}_{-0.3}$	$0.41^{+0.04}_{-0.04}$	$0.48^{+0.04}_{-0.05}$
E_b (TeV)	$0.03^{+0.8}_{-0.02}$	$0.019^{+0.007}_{-0.007}$	$0.05^{+0.007}_{-0.006}$	$0.04^{+0.006}_{-0.006}$	$0.06^{+0.03}_{-0.02}$	$0.05^{+0.02}_{-0.01}$
E_c (TeV)	25.0^{+30}_{-13}	50.0^{+40}_{-20}	$17.0^{+10.1}_{-5.4}$	$18.1^{+9.2}_{-6.3}$	$10.9^{+2.3}_{-0.7}$	$13.3^{+8.5}_{-2.7}$

Conclusions

- We found that that the SSC adequately explains the GRB afterglow emission from GRB 190114C, GRB 221009A, GRB 180720B amd GRB 190829A in the sub-GeV to TeV band, even though we accounted for EC emission. For both GRBs the SSC flux contributes majority of the combined (SSC and EC) flux to the total flux, since the EC flux was significantly lower than the SSC by two orders of magnitude. Thus the EC is negligible in these GRBs regardless of the scenario chosen.

- **GRB 190114C:** wind scenario produces a slightly better fit to the data at later times, with the best-fit parameter values being comparable for both scenarios.

- **GRB 221009A:** wind scenario fits the data slightly better, however no clear distinction can be made which one is preferred. The model, irrespective of the environment chosen, overpredicts the radio afterglow, thus suggesting that the component powering the low-frequency radio emission is not contributing to the optical and x-ray flux. The best-fit parameter values are comparable for both scenarios.

- **GRB 180720B**: wind scenario is the only preferred scenario. Some epochs can be fitted well. Our previous work (Barnard et al. 2024) we fit the VHE with EC, although not the case in this model. Degeneracy between models.

- **GRB 190829A**: ISM scenario is the only preferred scenario.

- ***Future prospects:*** Consider incorporating a wing like configuration (including the reverse shock) in the structured jet (see [16]), since low-energy multiwavelength afterglow is mainly governed by the synchrotron radiation from the forward and reverse shocks of the wing component. Also, a distinctive transition between the burst environments, from uniform to wind-like as done by Ren et al., (2024) is worth exploring to fit the higher frequency data better for some epochs.

Questions

Corner plots

GRB 190114C - ISM

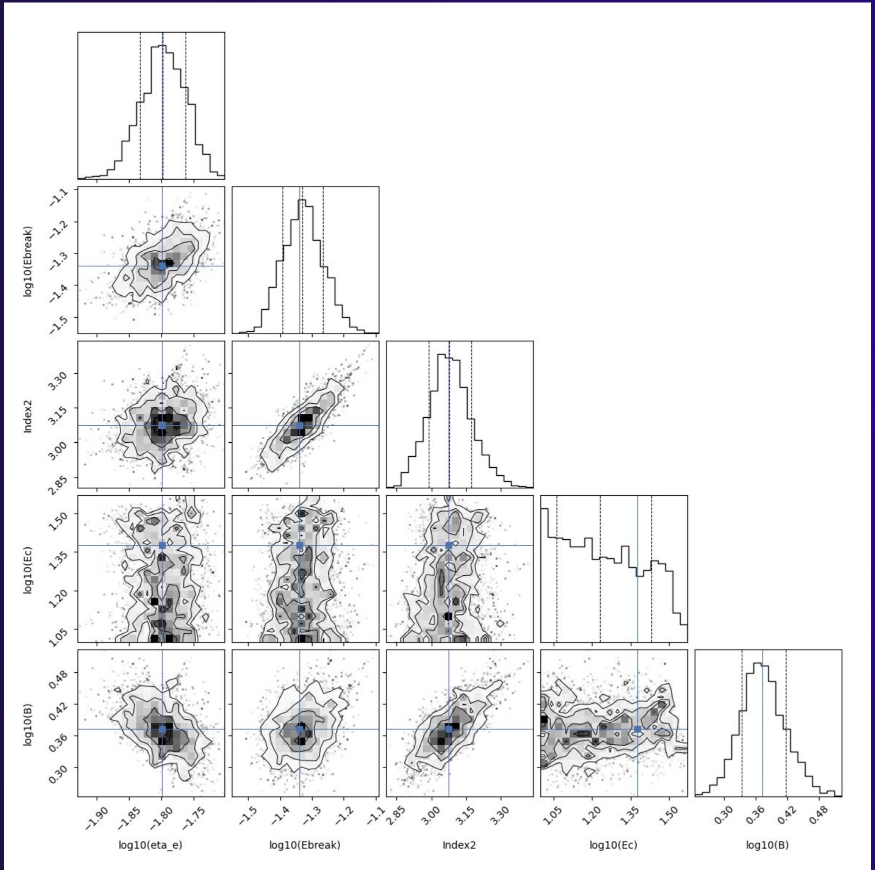

GRB 190114C - wind

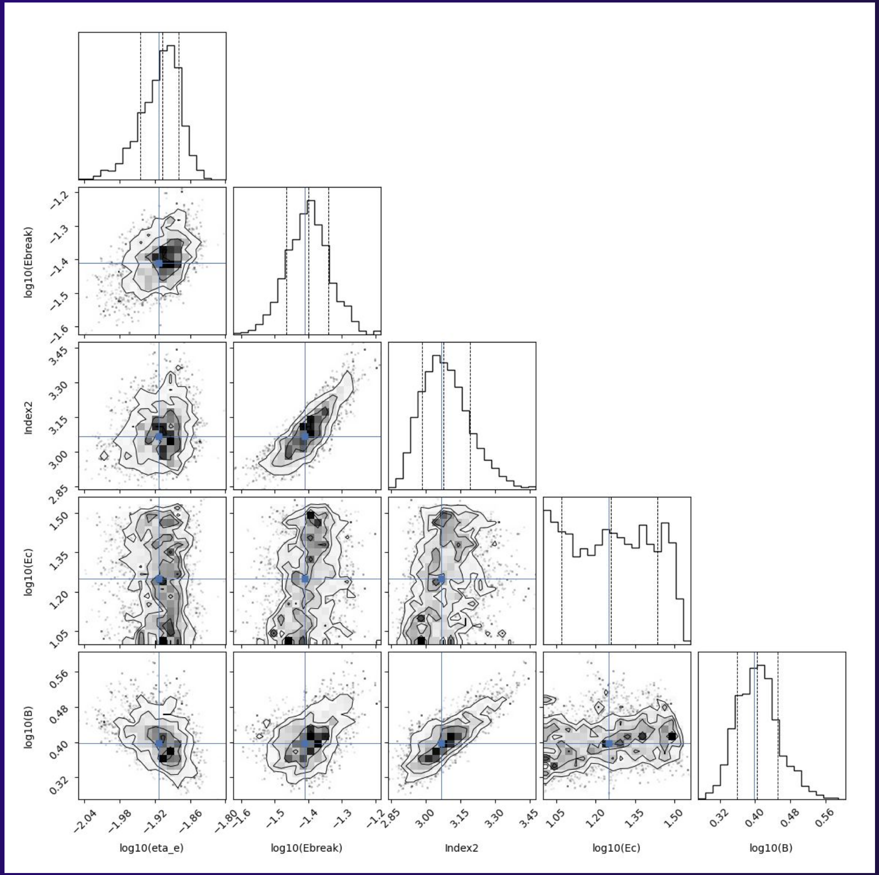

GRB 221009A - ISM

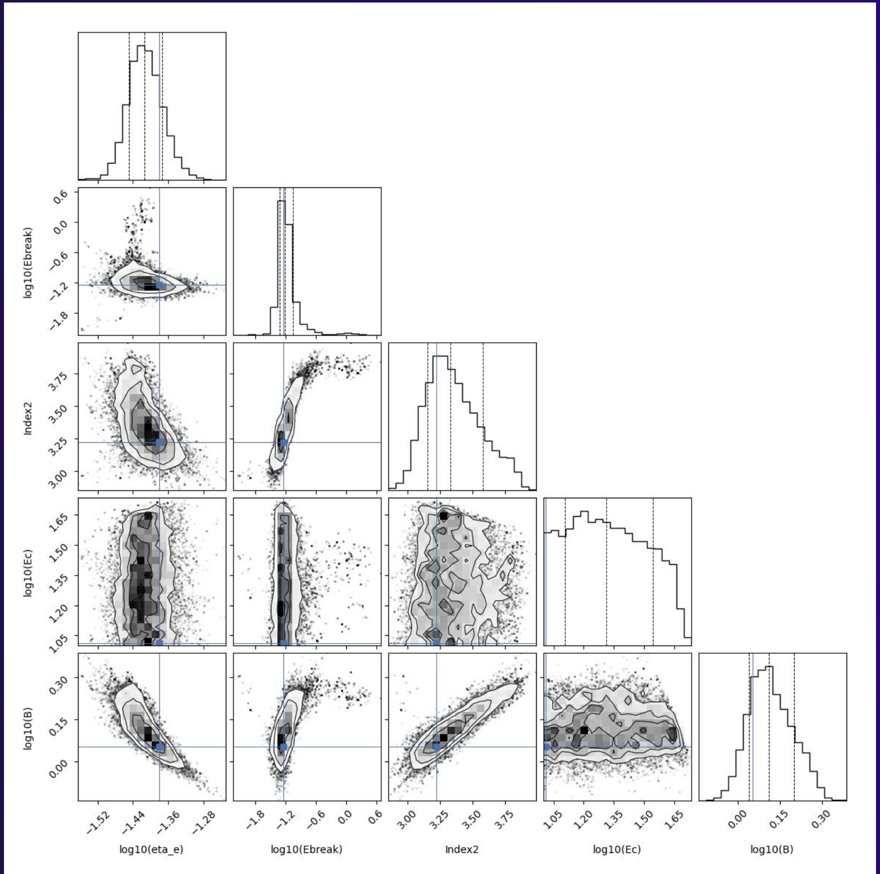

GRB 221009A - wind

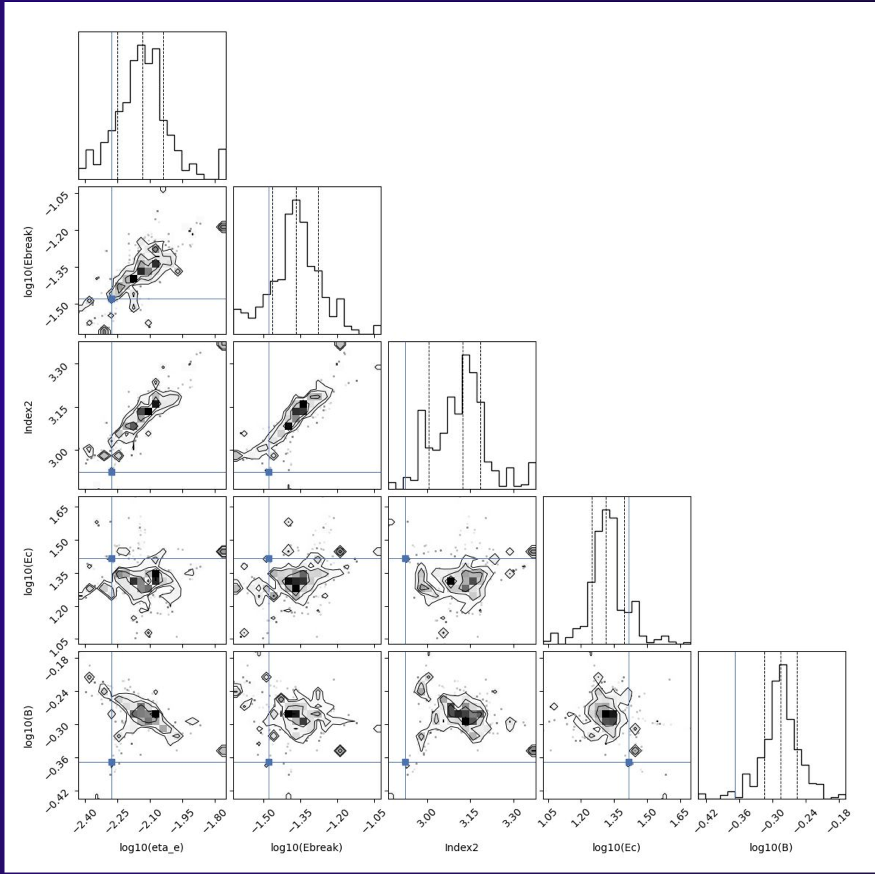

GRB 190829A - ISM

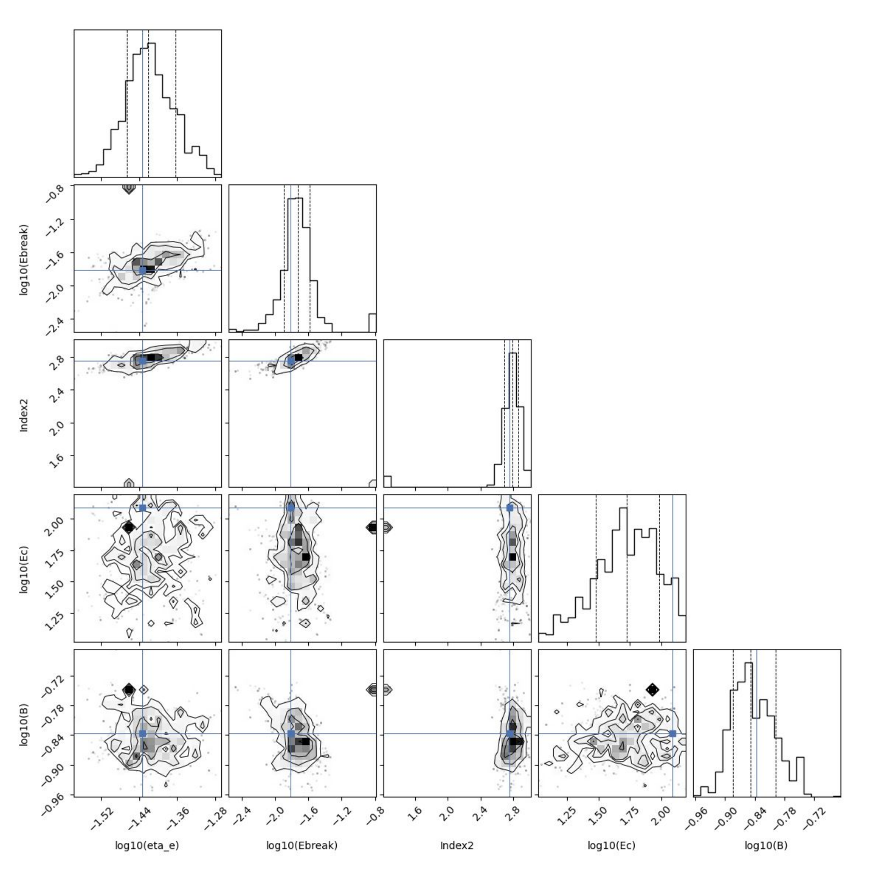

GRB 180720B - wind